Cell, Vol. 84, 105–114, January 12, 1996, Copyright ©1996 by Cell Press

Reconstitution In Vitro of the Motile Apparatus from the Amoeboid Sperm of Ascaris Shows That Filament Assembly and Bundling Move Membranes

Joseph E. Italiano, Jr.,* Thomas M. Roberts,* Murray Stewart,† and Carolyn A. Fontana*
*Department of Biological Science
Florida State University
Tallahassee, Florida 32306
†Medical Research Council Laboratory of Molecular Biology
Hills Road
Cambridge CB2 2QH
United Kingdom

Summary

We have developed an in vitro motility system from Ascaris sperm, unique amoeboid cells that use filament arrays composed of major sperm protein (MSP) instead of an actin-based apparatus for locomotion. Addition of ATP to sperm extracts induces formation of fibers ~2 μm in diameter. These fibers display the key features of the MSP cytoskeleton in vivo. Each fiber consists of a meshwork of MSP filaments and has at one end a vesicle derived from the plasma membrane at the leading edge of the cell. Fiber growth is due to filament assembly at the vesicle; thus, fiber elongation results in vesicle translocation. This in vitro system demonstrates directly that localized polymerization and bundling of filaments can move membranes and provides a powerful assay for evaluating the molecular mechanism of amoeboid cell motility.

Introduction

Amoeboid cell motility plays an important role in such diverse processes as macrophage migration and tumor metastasis. This type of locomotion requires extension of a motile pseudopod to pull the cell forward, a process typically attributed to modulation of an actin-based cytoskeleton (reviewed by Condeelis, 1993; Stossel, 1993; Oliver et al., 1994). The protrusive activity at the leading edge of these cells coincides with localized polymerization and cross-linking of actin filaments into meshworks or bundles and the concerted retrograde flow of these arrays away from the advancing front (reviewed by Lee et al., 1993; Theriot and Mitchison, 1992; Heath and Holifield, 1991).

Owing in large part to its complexity, the mechanism by which the actin cytoskeleton produces protrusion and locomotion is still uncertain. In addition to locomotion, actin is often engaged in other cellular functions such as shape determination, phagocytosis, movement of vesicles and organelles, surface rearrangements, and cytokinesis. Each of these activities requires a set of actin-binding proteins, and single cells often contain many such proteins with overlapping or redundant functions. This combination of functional versatility and biochemical complexity has made it difficult to define the components and properties that are essential to locomotion (reviewed by Condeelis, 1993).

The simplicity and specialization of the crawling sperm of nematodes such as Ascaris suum can offer advantages for investigating the mechanism of amoeboid motility (reviewed by Roberts and Stewart, 1995). Like conventional amoeboid cells, Ascaris sperm crawl by extending a pseudopod that undergoes localized protrusion, membrane ruffling, and cytoskeletal flow. In these cells, however, the role usually assigned to actin has been taken over by major sperm protein (MSP), a 14 kDa sperm-specific protein that forms a system of filaments that packs the pseudopod (Sepsenwol et al., 1989; Roberts and King, 1991; King et al., 1992). The MSP cytoskeleton is organized into 15–20 branched meshworks of densely packed filaments, called fiber complexes, that are assembled at leading edge of the pseudopod and flow rearward to the cell body, where they disassemble. The rate of sperm locomotion is coupled to the rate of assembly and flow of these fiber complexes (Roberts and King, 1991; Royal et al., 1995), suggesting that in nematode sperm, as in actin-based amoeboid cells, filament polymerization and bundling generate localized protrusion.

Because the motile behavior of Ascaris sperm so closely parallels that of actin-rich crawling cells, it is extremely likely that the physical principles underlying MSP- and actin-based crawling are the same. Ascaris sperm are highly specialized cells in which the MSP apparatus is dedicated almost entirely to locomotion. Therefore, many of the other properties of actin-based cytoskeletons have been dispensed with, and so the role of the MSP system in locomotion can be investigated without the complications imposed by a multifunctional cytoskeleton.

In this study, we describe a simple method to reconstitute in vitro the MSP cytoskeleton and its association with the leading edge of the pseudopod. We show that localized polymerization and bundling of MSP filaments can be harnessed to move plasma membrane–derived vesicles in much the same way as assembly of the fiber complexes appears to move the pseudopodial plasma membrane in vivo. We found that in addition to MSP movement requires components from the membrane at the leading edge of the cell and at least one other cytoplasmic factor.

Results

Movement Can Be Reconstituted with Sperm Cytosol and Membrane Vesicles

Ascaris sperm, like other amoeboid cells, advance over the substrate by pushing their pseudopod forward. This process appears to be driven by continuous assembly of fiber complexes along the plasma membrane at the leading edge of the pseudopod (Figure 1; see also Sepsenwol et al., 1989; Roberts and King, 1991; Royal et

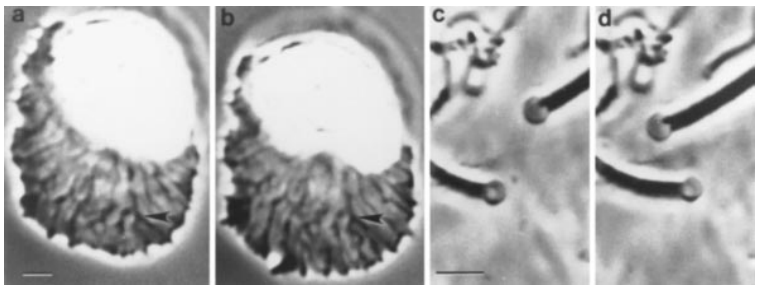

Figure 1. Localized Assembly of MSP Filament Arrays In Vivo and In Vitro

Computer-enhanced phase–contrast micrographs showing the elongation of fiber complexes at the leading edge of the pseudopod of a crawling sperm (a and b) and of fibers assembled in vitro by addition of ATP to S100 (c and d). The interval between frames was 10 s in both sequences. The arrows in (a) and (b) indicate a branch in a fiber complex. The portion of the fiber complex distal to the branch elongated in concert with protrusion of the leading edge. Likewise, the two prominent fibers in (c) and (d) elongated (in this case, at 35 μm/min) pushing their associated vesicles forward. Scale bars, 5 μm.

al., 1995). We report here the reconstitution of an in vitro system that retains the key features of this motile apparatus.

When we added ATP to the 100,000 × g supernatant (S100) obtained from frozen–thawed sperm, polymerization and bundling of MSP filaments produced elongating multifilament meshworks, or fibers, up to 2 μm in diameter. The growth of these fibers could be monitored in real time by computer-enhanced phase–contrast video microscopy (Figure 1). Each fiber had a membrane vesicle at one end that was pushed forward as the fiber grew. The rate of fiber elongation was rather variable and ranged from 2–35 μm/min (mean, 12 ± 4 μm/min; $n = 33$). The maximum rate of fiber growth was comparable to the average velocity of sperm crawling on glass coverslips (Royal et al., 1995). Growth continued for 90–120 min, with no detectable disassembly, to yield fibers that ranged from straight or gently curved to tight spirals or helices (Figure 2a). Individual fibers altered their pattern of growth as they elongated but, once formed, exhibited little or no change in shape or length. There was no correlation between the rate of elongation and the diameter of either the fiber or associated vesicle. Fibers labeled uniformly with antibody AZ10 (Figures 2b and 2c), a monoclonal antibody that binds specifically to MSP (Sepsenwol et al., 1989). Assembly required at least 0.1 mM ATP; ATP concentrations above this threshold did not enhance either the rate or duration of fiber growth. Fibers were not produced by other nucleotides, such as GTP or ADP, or by nonhydrolyzable analogs of ATP, including ATPγS and AMP–PNP.

Fractionation of diluted S100 by high speed centrifugation produced a supernatant composed of soluble cytosolic sperm proteins and a pellet that contained primarily membrane vesicles as judged by electron microscopy (EM) of thin sections of embedded samples. The supernatant failed to produce fibers in the presence of ATP either alone or when supplemented with purified MSP at 4 mM, its concentration in S100. However, fibers were formed when the pellet and the supernatant were recombined, indicating that assembly required components from both fractions. Addition of the same pellet to 4 mM MSP failed to produce fibers visible by light microscopy or polymerization of individual filaments detectable by either EM or sedimentation assays, indicating that the supernatant contains factors in addition to MSP that are essential for polymerization under these conditions. We also investigated the effect on the rate of movement of diluting S100 with KP buffer. As illustrated in Figure 2d, dilution 1:1 with buffer produced neglible changes in fiber growth rate, but higher dilutions resulted in a progressive reduction in the growth rate. At dilutions greater than 1:25, we could no longer detect any fiber formation. Significantly, when S100 was diluted with buffer containing 4 mM MSP (to keep the MSP concentration constant), the same decrease in the rate of fiber elongation was observed (Table 1). This indicated that the rate-limiting step of fiber growth involved some component of the S100 fraction in addition to MSP. This component does not appear to be a small molecule. We centrifuged a sample of S100 on a 5000 nominal molecular weight cut-off filter until approximately one third of the volume had passed through. We then tested both the filtrate and the residual unfiltered material for their ability to restore fiber growth rate when added to a mixture of membranes and either 1:10 or 1:25 diluted S100. At both dilutions, the residual material from above the filter restored fiber growth rate whereas the filtrate did not.

Localized Polymerization and Bundling of MSP Filaments Moves Vesicles

To investigate the pattern of fiber growth in greater detail, we examined fibers at an early stage of assembly so that we could monitor both ends of a fiber simultaneously. Figure 3 shows a time-lapse sequence of a fiber assembled in dilute S100 to slow the rate of elongation. As the fiber elongated, the thickened end distal to the membrane vesicle maintained its position relative to a stationary marker in the field. The vesicle, by contrast, moved to the right as the fiber grew. This pattern of elongation appeared to result from assembly of filaments at the vesicle-associated end of the fiber. However, addition of material elsewhere along the fiber could produce a similar pattern if one end of the fiber was attached to the substrate while the other was free. The behavior of fibers with bent shafts allowed us to distinguish between these possibilities (Figure 3b). In each bent fiber examined, elongation resulted in an increase in the distance between the bend and the vesicle-associated end of the fiber while the bend stayed stationary relative to the substrate. Thus, fiber elongation must be due to assembly at or at least very close to the membrane vesicle.

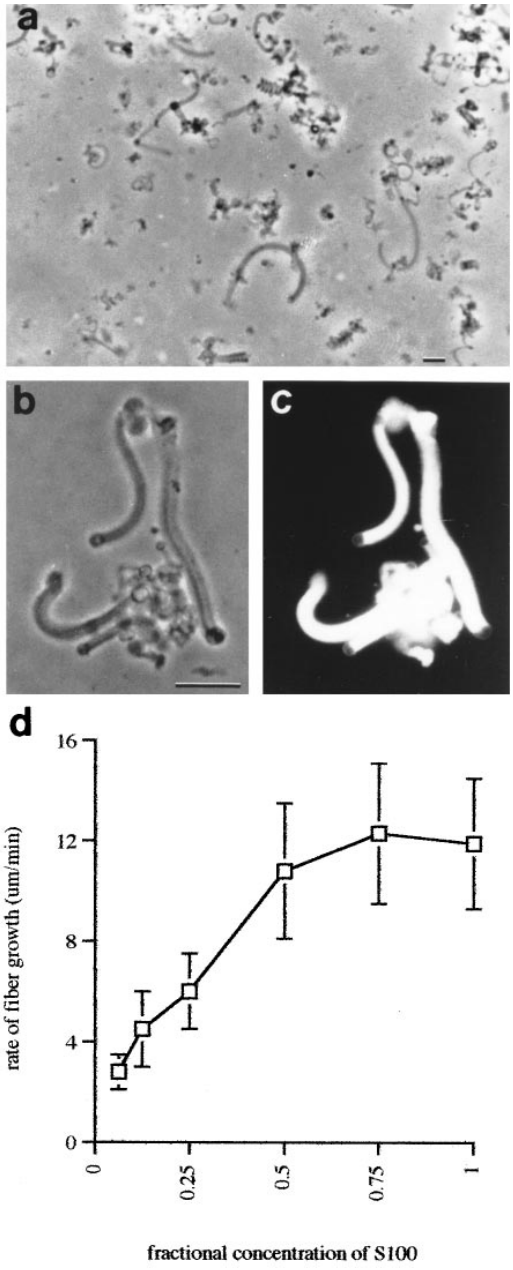

Figure 2. In Vitro Assembly Yields Fibers of Various Shapes That Label with Anti-MSP Antibody

(a) A panoramic view of a field of fibers shows the variety of shapes and sizes observed in a typical preparation. (b and c) Paired phase–contrast and fluorescence micrographs of fixed fibers labeled with anti-MSP monoclonal antibody AZ10 and observed by indirect immunofluorescence. Scale bars, 10 μm. (d) Variation in the rate of fiber growth as a function of dilution of S100 with KP buffer. Each point represents the mean of three trials, each of which included measurement of at least ten fibers. The bars are standard error of the mean.

Fibers assembled in vitro consisted of a dense meshwork of filaments that extended from an unordered region at one end, which differed in shape in each fiber, to the base of the associated vesicle at the opposite end (Figure 4). The shaft of each fiber was roughly cylindrical in cross section, and longitudinal grooves could often be observed by both light microscopy (see Figure 3) and scanning EM (SEM) (Figure 4). Few filaments extended out from the shaft of the fiber. Light microscopy indicated that a vesicle was present at the end of each fiber. We confirmed this observation at higher resolution by examining four preparations by SEM and did not ever observe a fiber without a vesicle at one end nor an example in which there was a discernible gap between the vesicle and the fiber that would be expected if the vesicle attached to the fiber loosely or transiently. Instead, the vesicles always abutted the filament meshwork. The vesicles were roughly spherical, and some contained additional vesicles or amorphous granular material. When growing fibers were treated with 1% Triton X-100, the vesicles could no longer be observed by light microscopy, indicating that the membranes had been solubilized. SEM of these extracted fibers showed a cup-shaped depression at one end (Figure 4c).

Table 1. Comparison of Fiber Growth Rate in S100 Diluted with KP Buffer versus Dilution with KP Buffer plus 4 mM MSP

	Fiber Growth Rate (μm/min)	
Dilution	KP Buffer	KP Buffer Plus 4 mM MSP
1:1	16.5 ± 3.1 (9)[a]	16 ± 3.6 (6)
1:10	3.1 ± 1.8 (7)	2.4 ± 0.5 (7)
1:20	1.9 ± 0.5 (8)	2.0 ± 0.7 (9)
1:30	0[b]	0

[a] Entries are mean ± standard deviation (number of fibers measured).
[b] Fiber growth could not be detected with or without added MSP.

Fiber-Associated Vesicles Are Derived from the Pseudopodial Plasma Membrane

Light microscopy indicated that only a very small fraction (<1%) of the vesicles in S100 were associated with fibers. The membrane systems of nematode sperm are well characterized (Ward et al., 1983). They lack an endoplasmic reticulum, Golgi, and lysosomes but in addition to their plasma membrane and mitochondria also contain membranous organelles (that become in-pockets of the cell body surface by fusing with the plasma membrane late in sperm development and are not found in the pseudopod) and a population of small vesicles concentrated at the cell body–pseudopod junction.

Immunofluorescence using an antiserum that stained only the surface of the cell indicated that the fiber-associated vesicles derived from the plasma membrane (Figure 5). This antiserum produced uniform labeling of the plasma membrane, but no labeling of internal organelles, in indirect immunofluorescence assays of fixed, detergent-permeabilized sperm (Figure 5b). Identical treatment of fibers resulted in specific labeling of the fiber-associated vesicles but not of the fiber itself (Figure 5f).

The labeling pattern obtained with an antibody directed against phosphotyrosine pinpointed the source of the fiber-associated vesicles to the leading edge of the pseudopodial plasma membrane. In indirect immunofluorescence assays, this antibody selectively labeled

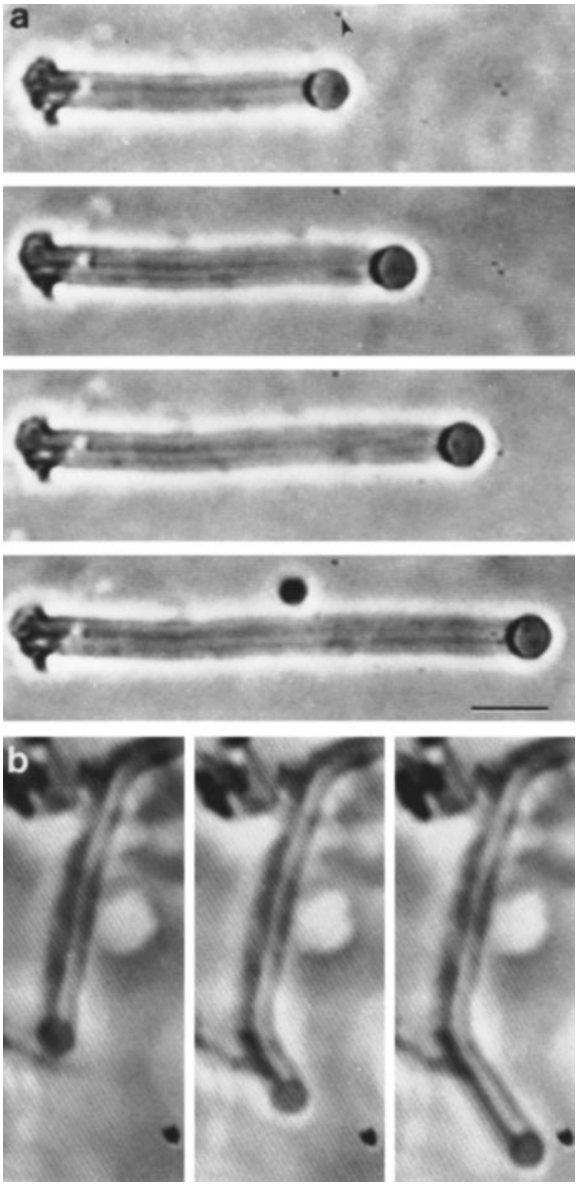

Figure 3. Assembly at the Vesicle Produces Fiber Elongation

(a) Sequence showing the early stages of growth of a fiber (interval between frames is 4 min). As the fiber elongates, it pushes its associated vesicle past a substrate-attached particle (arrowhead) while the opposite, thickened end remains stationary. Scale bar, 5 μm.

(b) Sequence showing the growth of a fiber with two bends. Note that, as the fiber elongated, the distance between the vesicle and the lower bend increased, but that the bend remained stationary relative to the substrate and its distance from the upper bend did not change. These fibers were assembled in 1:20 diluted S100 so that, compared with that of the fiber shown in Figure 1, their rate of growth was slowed, which facilitated more precise observation of elongation. Scale bar, 5 μm.

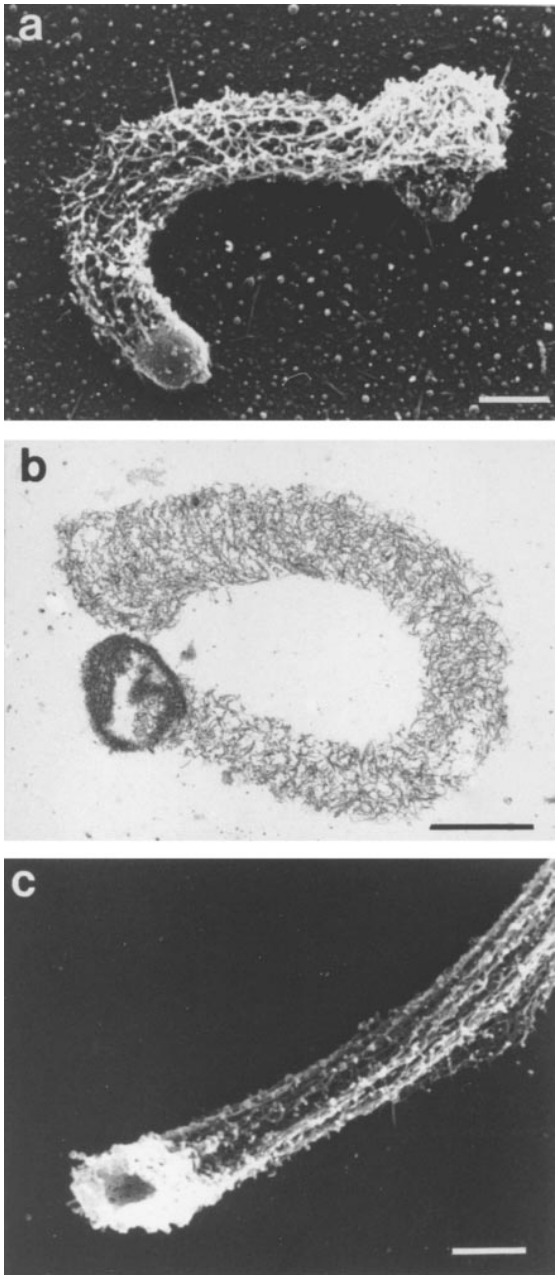

Figure 4. Fibers Are Meshworks of MSP Filaments

(a) SEM of a fixed fiber, prepared by the critical point method of Ris (1985), showing the meshwork arrangement of filaments.

(b) Transmission EM of a thin section through a fiber.

(c) SEM of a fiber treated with 1% Triton X-100 for 1 min before fixation. This treatment lysed the vesicle leaving a cup-shaped depression at the end of the fiber. Note the longitudinal grooves along the shaft of the fiber.

Scale bars, 1 μm.

the leading edge of the pseudopod of detergent-permeabilized sperm and also labeled the vesicles at the end of fibers assembled in vitro (Figure 6). In the latter case, the antibody produced a ring of fluorescence around the entire vesicle, and labeling was clearly not restricted to the vesicle–fiber interface. We were unable to detect labeling of any of the other vesicles in these preparations with the anti-phosphotyrosine antibody, suggesting that the presence of phosphotyrosylated proteins may determine whether a vesicle is competent to assemble fibers.

Fibers Still Assemble When Vesicle Membranes Are Removed by Detergent

To determine whether MSP polymerization and fiber formation require intact membrane vesicles, we treated the

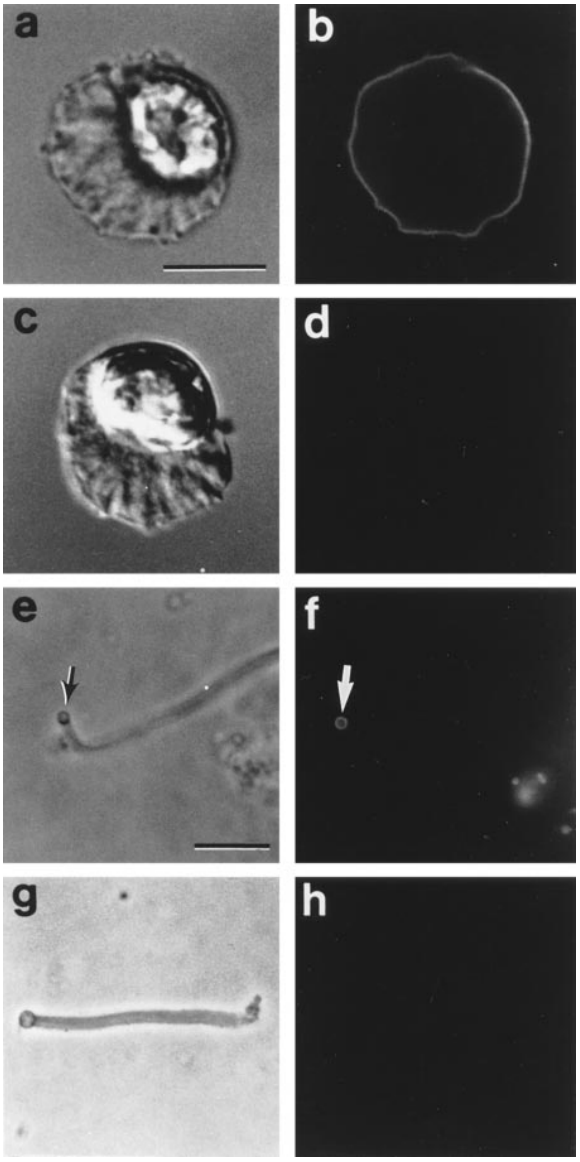

Figure 5. Fiber-Associated Vesicles Label with an Antiserum That Binds to the Sperm Plasma Membrane

Paired light (a, c, e, and g) and fluorescence (b, d, f, and h) micrographs showing indirect immunofluorescence labeling obtained with an antiserum raised against deglycosylated sperm membranes.
(a and b) Fixed, Triton X-100-permeabilized sperm probed with anti-membrane antiserum followed by FITC-conjugated anti-rabbit IgG. The plasma membrane was labeled uniformly, but there was no detectable labeling of any internal organelles.
(c and d) Control in which the primary antiserum was omitted.
(e and f) Fixed, permeabilized fiber labeled in the same way as the cell shown in (a) and (b). The fiber-associated vesicle (arrows) exhibits a ring of fluorescence, but the fiber itself is unlabeled.
(g and h) Control with the antiserum omitted.
Scale bars, 10 μm.

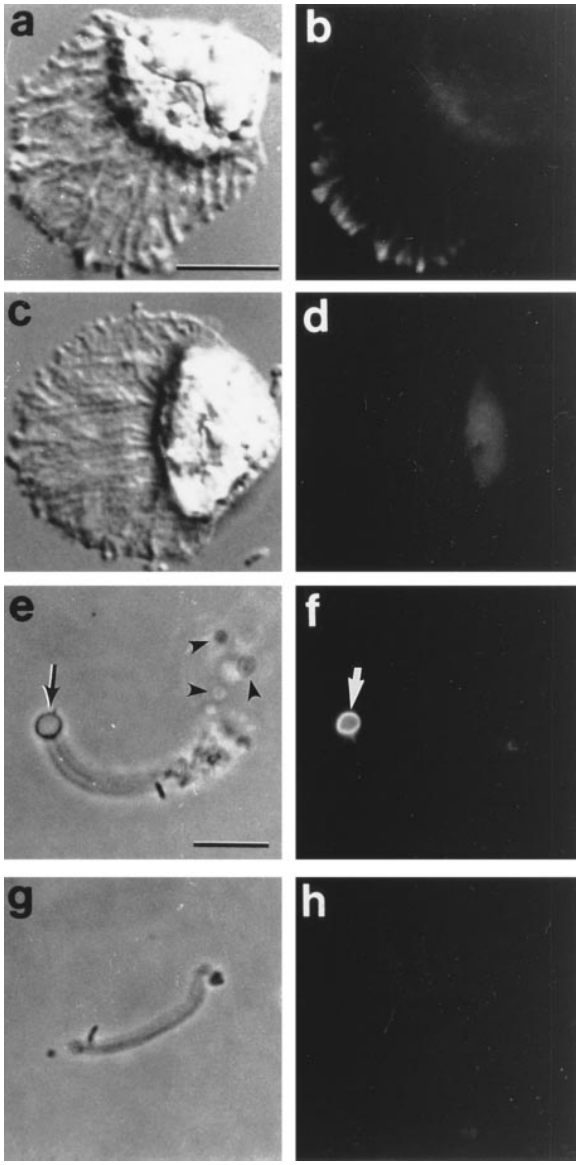

Figure 6. Anti-Phosphotyrosine Antibody Labels Both the Leading Edge of the Pseudopod and Fiber-Associated Vesicles

Crawling sperm (a and b) fixed, permeabilized with Triton X-100, and probed with anti-phosphotyrosine antibody followed by FITC-conjugated anti-rabbit IgG. The antibody labeled the leading edge of the pseudopod. The faint fluorescence at the cell body–pseudopod junction was also observed in control cells (c and d) in which the primary antibody was omitted. Anti-phosphotyrosine also selectively labeled fiber-associated vesicles (arrows in [e] and [f]) but not nearby free vesicles (arrowheads). Permeabilization was not required to obtain labeling of vesicles on fibers. No binding was detected on control fibers probed with secondary antibody alone. Scale bars, 10 μm.

pellet harvested by dilution and centrifugation of S100 with 1% Triton X-100. Intact vesicles were no longer detectable by light microscopy after detergent treatment. The supernatant obtained after centrifugation of this material induced the assembly of fibers similar to those assembled on vesicles (Figure 7a) when added to diluted, vesicle-free S100. Examination by SEM showed that, in addition to fibers, the Triton X-100-extracted pellet produced flattened meshworks of filaments (Figure 7b). Also, the fibers in these preparations had numerous filaments extending laterally from the shaft, and we were unable to detect membrane fragments at their ends. However, like their vesicle-associated counterparts, the fibers assembled in detergent-soluble membrane extracts labeled heavily at one end for phosphotyrosine (Figures 7c and 7d). Because these fibers

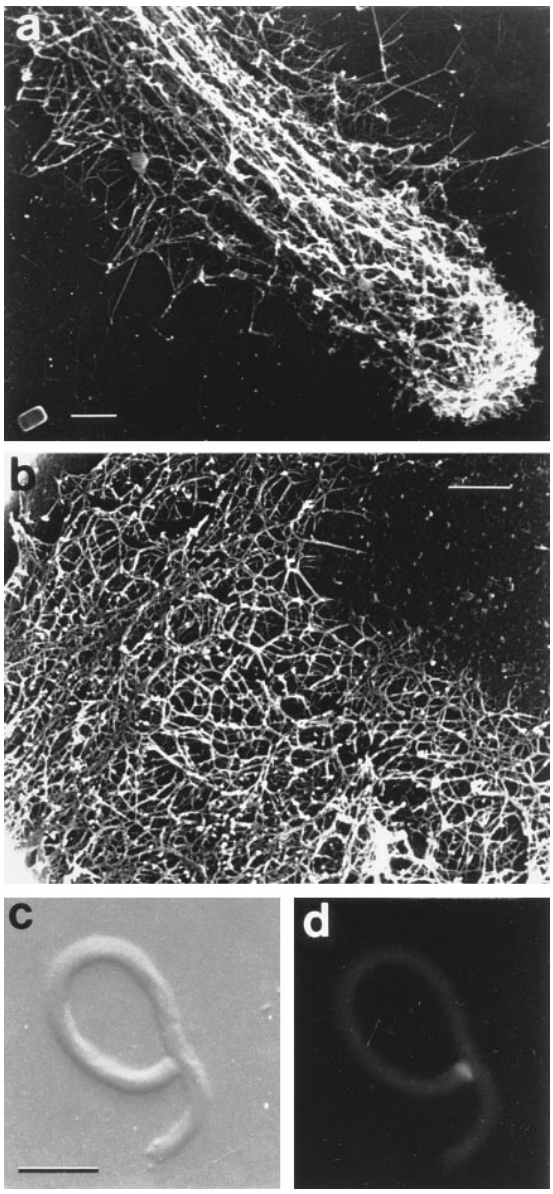

Figure 7. Triton X-100-Soluble Membrane Extract Induces Filament Assembly and Fiber Formation

Polymerization was initiated by combining the vesicle-free high speed supernatant of 1:20 diluted S100 with the soluble fraction obtained after treatment of the membrane fraction with 1% Triton X-100.

(a) SEM of a fiber with numerous filaments extending out from the shaft. Note the absence of a vesicle at the end of the fiber.

(b) SEM of a portion of a mat of filaments that also formed under these assembly conditions.

(c and d) Differential interference contrast and fluorescence micrographs of a fiber labeled with anti-phosphotyrosine by indirect immunofluorescence. One end of the fiber is heavily labeled although a vesicle is lacking.

Scale bars, 1 μm in (a) and (b), 10 μm in (c).

adhered poorly to the substrate, we were unable to follow the growth of individual fibers then fix and label to determine whether the growing end bound anti-phosphotyrosine. However, some of these fibers branched as they elongated. When we probed such fibers, the antibody labeled the end of each branch, indicating that, as observed in vesicle-associated fibers and the leading edge of the pseudopod of crawling cells, anti-phosphotyrosine selectively recognized the site of localized filament assembly.

This association of phosphotyrosylated proteins with the growing end of fibers both in the presence and absence of intact vesicles prompted us to test the effects of a battery of protein tyrosine kinase inhibitors on MSP polymerization. However, we were unable to inhibit fiber formation in vitro or in vivo with the kinase inhibitors herbimycin (0.4 μg/ml), genistein (10 μg/ml), or tyrphostins A1 (10 μg/ml), A25 (3 μg/ml), B42 (1.5 μg/ml), B44 (15 μg/ml), B50 (15 μg/ml), B46 (1.5 μg/ml), B48 (1.5 μg/ml), and B56 (1.5 μg/ml). Moreover, the vesicles on fibers assembled in the presence of these inhibitors labeled as intensely with anti-phosphotyrosine antibody as the vesicles on fibers assembled without inhibitors, indicating that these agents did not block tyrosine phosphorylation in this system.

Discussion

To understand the mechanism of amoeboid locomotion, we need to identify the molecular machinery underlying the protrusive activity of the leading edge. In both actin- and MSP-based systems, this process is associated with localized assembly and bundling or cross-linking of filaments into networks. By reconstituting in vitro a system that retains key elements of the motile apparatus of nematode sperm, we have established a basis for investigating the mechanism of amoeboid cell motility and also an assay system to detect its other components. In this study, we have shown that membrane components isolated from the leading edge of the sperm pseudopod trigger the assembly of MSP filament meshworks in vitro and that this process can be harnessed to drive the movement of vesicles. This system, therefore, provides a strikingly direct demonstration that fiber assembly and bundling can move membranes.

Components Required for Reconstitution of the Motile Apparatus

The results obtained with the in vitro assembly system indicated that at least four components are involved in fiber formation and associated vesicle locomotion.

MSP

Ascaris sperm lack significant quantities of actin and tubulin, and the only filament-forming protein present in any quantity is MSP, which forms the major constituent of the fibers. In the in vitro system, MSP polymerization keeps pace with the rate of vesicle translocation, which averages 0.2 μm/s and can be as rapid as 0.6 μm/s. The macromolecular structure of MSP filaments is known in outline: filaments are constructed from two subfilaments wrapped around one another in right-handed helical tracks of pitch 22.5 nm. The subfilament helices are left-handed and have a pitch near 9 nm; they appear to contain 16 MSP molecules in five helical turns (Stewart at al., 1993, 1994; King et al., 1994b). Thus, the axial spacing between MSP monomers along a subfilament is probably on the order of 3 nm. From this we

can estimate the approximate rate at which subunits are added onto filaments. If the filaments in fibers were oriented parallel to the path of vesicle movement, addition of ~200 subunits per second would be required to account for the observed mean rate of fiber elongation and ~600 subunits per second for the maximum rate observed. Fibers, however, contain meshworks of filaments oriented at various angles relative to the axis of elongation. Therefore, the rate of subunit addition must be more rapid by perhaps as much as a factor of 2. This would give a rate of elongation of ~400 subunits per second for the mean and ~1200 for the maximum fiber elongation rate. Given a cytoplasmic concentration of MSP of 4 mM, this would imply a k_{on} of 0.1 $\mu M^{-1}s^{-1}$ for the mean growth rate and a maximum k_{on} of 0.3 $\mu M^{-1}s^{-1}$. These estimated rates of addition for MSP are slower than the measured on rates for actin (Pollard, 1986). Consequently, the rate of MSP polymerization observed in these cellular extracts in not unusually high and so does not require some novel mechanism.

Membrane Components

S100 only formed fibers when either membrane-bound vesicles or their detergent-extracted components were present. Thus, MSP polymerization under these conditions requires specific components from the plasma membrane, although an intact bilayer is not essential. Immunolabeling revealed two important features of the membrane vesicles that support fiber assembly. First, these vesicles derive from the leading edge of the pseudopod, the only membrane region that labeled with both anti-membrane antiserum and anti-phosphotyrosine antibody. Second, because anti-phosphotyrosine labeling requires permeabilization of sperm but not of the fiber-associated vesicles, the vesicles appear to be fragments of plasma membrane resealed inside out. Thus, the cytoplasmic surface of the membrane associated with filament assembly in vivo is exposed to participate in fiber formation in vitro. Although tyrosine phosphorylation was associated with fiber formation, we have not yet obtained direct positive evidence linking the two.

Cytosolic Factors

The failure of purified MSP to form fibers in the presence of membranes or to restore the rate of fiber formation when added to diluted S100 indicates that fiber formation involves one or more cytosolic components in addition to MSP. Such a factor could promote filament assembly or bundling. MSP filaments, however, have an intrinsic propensity to assemble into larger aggregates (King et al., 1994b) that is a consequence of their unique helical structure (Stewart et al., 1994) and so may not be as dependent as actin filaments on cross-linking proteins to form networks. Also, if the sole activity of the unknown component(s) of the S100 fraction was to form networks, we would have expected to detect assembly of individual filaments when vesicles were combined with purified MSP. Instead, we found that polymerization did not occur without S100, suggesting that cytosolic factors interact with membrane components to induce filament formation. The results of dilution assays underscored the importance of these factors. The decrease in fiber elongation rate with S100 dilution, even when the MSP concentration was kept constant, indicated that the rate of fiber growth was limited by the activity of a non-MSP component of the system rather than by the rate of association of MSP with the fiber.

ATP

The in vitro motility system demonstrated that the energy source for fiber elongation was ATP, which could not be substituted by other nucleotides such as GTP. Unlike the assembly of actin filaments and microtubules, the formation of MSP filaments does not appear to require nucleotide binding to the polymerizing unit. For example, the amino acid sequence of MSP does not contain a putative nucleotide-binding motif (King et al., 1992), and ATP is not required for the assembly of MSP into filaments in the presence of water-miscible alcohols (King et al., 1992, 1994b; Stewart et al., 1994). Moreover, preliminary assays by electron spin resonance failed to detect binding of ATP to MSP in solution (K_d of >300 mM; J. E. I. and P. Fajer, unpublished data). It appears, therefore, that the energy necessary for fiber formation and membrane movement is provided indirectly.

Comparison of Fiber Assembly In Vitro and Fiber Complex Formation In Vivo

The assembly of fibers in vitro shares several features with the construction of fiber complexes within the sperm pseudopod. Both are built by preferential addition of filament mass at their membrane-associated end. Moreover, the rates of elongation of fibers and fiber complexes are comparable, and both are composed of meshworks of MSP filaments. Although fiber assembly has been reconstituted in the in vitro system, the corresponding fiber disassembly that occurs in vivo has not. In crawling sperm there is a finely tuned balance between assembly and disassembly of the filament system at opposite ends of the pseudopod so that fiber complexes treadmill but exhibit little change in length as the cell progresses. Construction of fibers in vitro, by contrast, involves assembly at one end without concommitant disassembly at the other. The pseudopod exhibits a pH gradient from the leading edge to the base that appears to be involved in the spatial control of cytoskeletal dynamics (King et al., 1994a). We have not reconstituted this pH gradient in the in vitro system, and this may explain, at least in part, why fibers assembled in vitro do not show the same localized disassembly exhibited by the pseudopodial filament system.

Examination of cytoskeletal dynamics in intact sperm suggests that although disassembly is important for the treadmilling of fiber complexes and associated with locomotion as a whole, it is unlikely to be related to membrane protrusion, the primary focus of the present work. Further support for the key role of fiber assembly in protrusion comes from previous work that showed that treatment of sperm with weak acids causes reversible cytoskeletal disassembly. When these cells are washed, they recover by rebuilding fiber complexes along the pseudopod membrane. The initiation of cytoskeletal reassembly is sufficient to reform surface protrusions, but locomotion does not resume until the cytoskeleton is completely rebuilt and starts to treadmill (Roberts and King, 1991; King et al., 1994a).

Comparison to Actin-Based Systems

Several models have been proposed to explain the forces underlying protrusion in amoeboid cells (reviewed by Condeelis, 1992). Early ideas focussed on actomyosin contractility as the cause of protrusion but recent studies, particularly those involving myosin deletion mutants of Dictyostelium (DeLozanne and Spudich, 1987; Knecht and Loomis, 1987; Wessels et al., 1991; Titus et al., 1993), have suggested that myosin is more likely involved in fine-tuning protrusive activity than driving it. Localized polymerization of actin filaments is now thought to play a key role in protrusion (reviewed by Cooper, 1991; Condeelis, 1993; Zigmond, 1993; Cramer et al., 1994) and has also been implicated in other specialized forms of motility, such as the acrosome reaction in Thyone sperm (Tilney and Inoue, 1982), the movement of surface-attached polycationic beads on Aplysia neuronal growth cones (Forscher et al., 1992), and extension of filopodia by activated platelets (Hartwig, 1992). However, dissection of the relationship of actin polymerization to protrusion has been impaired by the complex and transient nature of the membrane–cytoskeletal interactions involved (Luna and Hitt, 1992). For example, Luna and colleagues (Shariff and Luna, 1990; Chia et al., 1993; Hitt et al., 1994) have shown that a single membrane protein, ponticulin, accounts for nearly all actin binding and nucleating activity of the Dictyostelium plasma membrane, yet, surprisingly, ponticulin-null mutants crawl efficiently. Molecular genetics approaches have begun to illuminate the roles of other actin-binding proteins in cell motility (see, for example, Cunningham et al., 1992; Cox et al., 1992) but have provided few insights about the precise role of polymerization in protrusion.

The pronounced similarity between MSP- and actin-based motility displayed at the level of whole-cell locomotion is also reflected in several features shared between the MSP in vitro system and the motility of intracellular bacteria such as Listeria monocytogenes and Shigella flexneri. These pathogens commandeer the host cytoskeleton to form an actin filament meshwork, or comet tail, that pushes the bacterium through the host cell cytoplasm (reviewed by Tilney and Tilney, 1993; Cossart and Kochs, 1994; Southwick and Purich, 1994). In both the MSP and bacterial systems, movement depends on assembly of filaments and their organization into a well-defined meshwork or tail. Moreover, the Listeria comet tail maintains a balance between filament assembly and disassembly much like the fiber complexes in the sperm pseudopod. Listeria requires the ActA surface protein whereas the MSP system requires a vesicle component, presumably a protein, that is not inactivated by Triton X-100 extraction. Listeria requires host cytoplasmic factors other than actin (Theriot et al., 1994; Pistor et al., 1995), and the in vitro MSP system also requires an additional cytoplasmic factor. Both systems appear to use energy indirectly, and both can be reconstituted in vitro (Theriot et al., 1994). The precise molecular mechanisms by which the actin-based Listeria and Shigella systems generate motion are not yet known, but nucleation release (Theriot and Mitchison, 1992) and thermal ratchet (Peskin et al., 1993) models have been proposed.

The close analogy between locomotion based on MSP- and actin-based motility indicates that, although the molecular components are different, similar mechanisms are likely to apply to both systems. In this regard, the Ascaris sperm-based in vitro system provides direct evidence that filament polymerization, bundling, or both can produce the force to move membranes. Moreover, the similarity in organization and growth of fibers assembled with solubilized membranes, and those built on vesicles suggested that the forces generated under both conditions are the same and that the membrane bilayer does not participate directly in force production. The observation that fibers can move membrane vesicles in vitro makes it very plausible that the fiber complexes can generate pseudopodial plasma membrane protrusion in vivo and, in turn, that analogous filament formation and bundling can produce protrusion in actin-based systems. Overall, the in vitro reconstitution of the MSP-based apparatus provides a powerful assay system for characterizing the components of the motile machinery of nematode sperm and identifying the forces they produce.

Experimental Procedures

Sperm Isolation and Manipulation

Ascaris males were collected from the intestines of infected hogs at Lykes Pork Processing (Moultrie, GA). Worms were transported to the laboratory in phosphate-buffered saline containing 10 mM $NaHCO_3$ (pH 7) at 37°C. Sperm were isolated by draining the contents of the seminal vesicle into tubes containing HKB buffer (50 mM HEPES, 65 mM KCl, 10 mM $NaHCO_3$ [pH 7.6]), washed, and treated with vas deferens extract, prepared according to the method of Sepsenwol et al. (1986), to trigger pseudopod formation and complete development into motile spermatozoa. These cells were used immediately or pelleted by 10 s centrifugation at 10,000 × g and stored at −70°C.

Preparation of Sperm Extracts for In Vitro Assembly

Sperm were lysed by two freeze–thaw cycles and then centrifuged at 100,000 × g for 1 hr at 4°C in a Beckman (Palo Alto, CA) TLA 100.3 rotor. The supernatant (S100) was either used for in vitro assembly assays or fractionated further by 20-fold dilution with 8 mM KH_2PO_4, 2 mM K_2HPO_4 (pH 6.7) (KP buffer) followed by centrifugation at 100,000 × g for 1 hr at 4°C. The resulting supernatant was harvested, and the pellet resuspended in a small volume of KP buffer. These fractions were stored at −70°C until use. For some experiments, the pellet was resuspended in KP buffer that contained 1% Triton X-100, incubated 15–30 min at room temperature, and centrifuged at 10,000 × g for 5 min. The detergent-soluble supernatant was either used immediately or stored at −70°C. Purified MSP used in selected assays was prepared as described by King et al. (1992). The MSP concentration in extracts was determined by comparison with Coomassie blue–stained SDS–PAGE gel lanes loaded with standards of known MSP concentration. To isolate the low molecular weight components of S100, 100 μl samples were loaded onto Millipore (Bedford, MA) ultrafree MC 5000 nominal molecular weight limit filter units and spun at 4°C in the matching Millipore centrifuge until approximately one third of the volume had passed through the filter. The filtrate and residual unfiltered material were collected and used immediately in fiber assembly assays.

Examination of Fiber Assembly by Light Microscopy

Fractions for in vitro assembly were mixed in 1.5 ml microcentrifuge tubes and pipetted into chambers with a volume of 18–20 μl formed by mounting a 22 × 22 mm glass coverslip onto a glass slide with two parallel strips of Scotch two-sided tape. All glassware was washed in ethanol before use. Preparations were examined on a Zeiss Axiovert microscope equipped with 100× neofluor/phase–

contrast and 100× differential interference contrast objectives. Images were obtained using a NEC (Elk Grove Village, IL) charged coupled device (CCD) camera, digitized, and processed by background subtraction and contrast enhancement using Image-1 software and hardware (Universal Imaging, West Chester, PA), and stored on videotape. Photographs of video images displayed on a Sony Trinitron monitor were recorded on Kodak TMAX-100 35 mm film as described by Inoue (1986).

EM

To prepare specimens for thin sectioning, live cells or fibers assembled in cell-free extracts were pipetted onto 4 × 4 mm ethanol-washed glass coverslips and fixed for 30 min in HKB buffer containing 1% glutaraldehyde, 0.2% tannic acid, plus 0.05% saponin (cells) or KP buffer containing 1.25% glutaraldehyde (fibers). Preparations were then washed, treated with 0.1% OsO_4 for 30 min, dehydrated through an ascending ethanol series followed by propylene oxide, and embedded in Polybed 812 resin (Polyscience, Incorporated, Warrington, PA). Thin sections were stained with 2.5% uranyl acetate in 50% methanol followed by lead citrate and examined in a JEOL 1200 EM operated at 80 kV.

For SEM, fibers assembled in vitro were pipetted onto coverslips and fixed for 30 min in 1.25% glutaraldehyde in KP buffer. After washing with KP buffer, samples were dehydrated in ethanol, critical point dried by the method of Ris (1985), coated with gold–palladium, and examined in a JEOL 840 SEM operated at 20 kV.

Immunofluorescence

Antibodies and Antiserum

Affinity-purified polyclonal anti-phosphotyrosine antibody was obtained from Transduction Laboratories (Lexington, KY). Antibody AZ10, a monoclonal antibody directed against MSP, was produced and purified as described by Sepsenwol et al. (1989). To prepare anti-membrane antiserum, the membrane-enriched fraction from sperm extracts, obtained as described above, was treated with 20 mM sodium periodate for 18 hr at 4°C in the dark to remove carbohydrate residues then washed by five cycles of centrifugation and resuspension in KP buffer. Initial immunization was by subcutaneous injection of a New Zealand white rabbit with 0.5 ml of packed membranes in complete Freund's adjuvant. A booster injection of membranes in incomplete Freund's adjuvant was administered 1 month later and the rabbit bled at weekly intervals. Whole blood was clotted and centrifuged, and the antiserum stored at −70°C until use. Secondary antibodies, fluorescein isothiocyanate (FITC) conjugates of goat anti-mouse immunoglobulin G (IgG) and anti-rabbit IgG, were obtained from Jackson Immunoresearch Laboratories (West Grove, PA). All antibodies were used at 5 μg/ml in KP buffer; anti-membrane antiserum was used at 1:100 dilution in the same buffer.

Labeling Procedures

Sperm or in vitro assembled fibers were pipetted into coverslip chambers, inverted to allow specimens to adhere to the coverslip, and fixed by perfusion with 1.25% glutaraldehyde in HKB (cells) or KP (fibers) buffer. When desired, fixed membranes were permeabilized by treatment with 0.5% Triton X-100 for 15 min. Specimens were washed, treated three times for 20 min with 10 mM $NaBH_4$ to quench unreacted aldehydes, and incubated in 0.1% bovine serum albumin for 2 hr to minimize nonspecific binding. The specimens were then incubated in primary antibody or antiserum for 2–6 hr, washed, treated with appropriate secondary antibody for 2 hr, and washed again. Controls were processed identically except for omission of the primary antibody or antiserum. Immunofluorescence labeling was examined under a 100× neofluor/phase–contrast objective on a Zeiss Axiovert microscope equipped with appropriate excitation and barrier filters for FITC fluorescence. Images were recorded on Kodak TMAX-100 35 mm film. For anti-phosphotyrosine, we also demonstrated that staining was eliminated by incubating 10 mM phosphotyrosine with the primary antibody.

Acknowledgments

We thank our colleagues in Tallahassee and Cambridge for many valuable suggestions and, in particular, Lawrence LeClaire and Julie Essig for expert technical assistance and Kim Riddle for help with light microscopy and EM. This work was supported by National Institutes of Health grant GM-29994.

Received August 24, 1995; revised October 27, 1995.

References

Chia, C.P., Shariff, A., Savage, S.A., and Luna, E.J. (1993). The integral membrane protein, ponticulin, acts as a monomer in nucleating actin assembly. J. Cell Biol. *120*, 909–922.

Condeelis, J. (1992). Are all pseudopods created equal? Cell Motil. Cytoskel. *22*, 1–6.

Condeelis, J. (1993). Life at the leading edge: the formation of cell protrusions. Annu. Rev. Cell Biol. *9*, 411–444.

Cooper, J.A. (1991). The role of actin polymerization in cell motility. Annu. Rev. Physiol. *53*, 584–605.

Cossart, P., and Kochs, C. (1994). The actin-based motility of the facultative intracellular pathogen *Listeria monocytogenes*. Mol. Microbiol. *13*, 395–402.

Cox, D., Condeelis, J., Wessels, D., Soll, D., Kern, H., and Knecht, D.A. (1992). Targeted disruption of the ABP-120 gene leads to cells with altered motility. J. Cell Biol. *116*, 943–955.

Cramer, L.P., Mitchison, T.J., and Theriot, J.A. (1994). Actin-dependent motile forces and cell motility. Curr. Opin. Cell Biol. *6*, 82–86.

Cunningham, C.C., Gorlin, J.B., Kwiatkowski, D.J., Hartwig, J.H., Janmey, P.A., Byers, H.R., and Stossel, T.P. (1992). Actin-binding protein requirement for cortical stability and efficient locomotion. Science *255*, 325–327.

DeLozanne, A., and Spudich, J.A. (1987). Disruption of the *Dictyostelium* myosin heavy chain gene by homologous recombination. Science *236*, 1086–1091.

Forscher, P., Lin, C.-H., and Thompson, C. (1992). Novel form of growth cone motility involving site-directed actin filament assembly. Nature *357*, 515–518.

Hartwig, J.H. (1992). Mechanisms of actin rearrangements mediating platelet activation. J. Cell Biol. *118*, 1421–1442.

Heath, J.P., and Holifield, B.F. (1991). Cell locomotion: new research tests old ideas on membrane and cytoskeletal flow. Cell Motil. Cytoskel. *18*, 245–257.

Hitt, A.L., Hartwig, J.H., and Luna E.J. (1994). Ponticulin is the major high affinity link between the plasma membrane and the cortical actin network in *Dictyostelium*. J. Cell Biol. *126*, 1433–1444.

Inoue, S. (1986). Video Microscopy (New York: Plenum Press).

King, K.L., Stewart, M., Roberts, T.M., and Seavy, M. (1992). Structure and macromolecular assembly of two isoforms of the major sperm protein (MSP) from the amoeboid sperm of the nematode, *Ascaris suum*. J. Cell Sci. *101*, 847–857.

King, K.L., Essig, J., Roberts, T.M., and Moerland, T.S. (1994a). Regulation of the *Ascaris* major sperm protein (MSP) cytoskeleton by intracellular pH. Cell Motil. Cytoskel. *27*, 193–205.

King, K.L., Stewart, M., and Roberts, T.M. (1994b). Supramolecular assemblies of the *Ascaris suum* major sperm protein (MSP) associated with amoeboid cell motility. J. Cell Sci. *107*, 2941–2949.

Knecht, D.A., and Loomis, W.F. (1987). Antisense RNA inactivation of myosin heavy chain gene expression in *Dictyostelium discoideum*. Science *236*, 1081–1085.

Lee, J., Ishihara, A., and Jacobson, K. (1993). How do cells move along surfaces? Trends Cell Biol. *3*, 366–370.

Luna, E.J., and Hitt, A.L. (1992). Cytoskeleton–plasma membrane interaction. Science *258*, 955–964.

Oliver, T., Lee, J., and Jacobson, K. (1994). Forces exerted by locomoting cells. Semin. Cell Biol. *5*, 139–147.

Peskin, C.S., Odell, G.M., and Oster, G.F. (1993). Cellular motions and thermal fluctuations: the Brownian rachet. Biophys. J. *65*, 316–324.

Pistor, S., Chakraborty, T., Walter, U., and Wehland, J. (1995). The bacterial actin nucleator protein ActA of *Listeria monocytogenes*

contains multiple binding sites for host microfilament proteins. Curr. Biol. *5*, 517–525.

Pollard, T.D. (1986). Rate constants for the reactions of ATP- and ADP-actin with the ends of actin filaments. J. Cell Biol. *103*, 2747–2754.

Ris, H. (1985). The cytoplasmic filament system in critical point dried whole mounts and plastic embedded sections. J. Cell Biol. *100*, 1474–1487.

Roberts, T.M., and King, K.L. (1991). Centripetal flow and directed reassembly of the major sperm protein (MSP) cytoskeleton in the amoeboid sperm of the nematode, *Ascaris suum*. Cell Motil. Cytoskel. *20*, 228–241.

Roberts, T.M., and Stewart, M. (1995). Nematode sperm locomotion. Curr. Opin. Cell Biol. *7*, 13–17.

Royal, D., Royal, M., Italiano, J., Roberts, T., and Soll, D. (1995). In *Ascaris* sperm pseudopods, MSP fibers move proximally at a constant rate regardless of the forward rate of cellular translocation. Cell Motil. Cytoskel. *31*, 241–253.

Sepsenwol, S., Nguyen, M., and Braun, T. (1986). Adenylate cyclase activity is absent in inactive and motile sperm of the nematode parasite, *Ascaris suum*. J. Parasitol. *72*, 962–964.

Sepsenwol, S., Ris, H., and Roberts, T.M. (1989). A unique cytoskeleton associated with crawling in the amoeboid sperm of the nematode, *Ascaris suum*. J. Cell Biol. *108*, 55–66.

Shariff, A., and Luna, E.J. (1990). *Dictyostelium discoideum* plasma membranes contain an actin-nucleating activity that requires ponticulin, an integral membrane protein. J. Cell Biol. *110*, 681–692.

Southwick, F.S., and Purich, D.L. (1994). Dynamic remodeling of the actin cytoskeleton: lessons learned from *Listeria* locomotion. Bioessays *16*, 885–891.

Stewart, M., King, K.L., and Roberts, T.M. (1993). Crystallization of the motile major sperm protein (MSP) of the nematode, *Ascaris suum*. J. Mol. Biol. *232*, 298–300.

Stewart, M., King, K.L., and Roberts, T.M. (1994). The motile major sperm protein (MSP) of *Ascaris suum* forms filaments constructed from two helical subfilaments. J. Mol. Biol. *242*, 60–71.

Stossel, T.P. (1993). On the crawling of animal cells. Science *260*, 1086–1094.

Theriot, J.A., and Mitchison, T.J. (1992). The nucleation-release model of actin filament dynamics in cell motility. Trends Cell Biol. *2*, 219–222.

Theriot, J.A., Rosenblatt, J., Portnoy, D.A., Goldschmidt-Clermont, P.J., and Mitchison, T.J. (1994). Involvement of profilin in the actin-based motility of L. monocytogenes in cells and cell-free extracts. Cell *76*, 505–517.

Tilney, L.G., and Inoue, S. (1982). Acrosomal reaction of *Thyone* sperm. II. The kinetics and possible mechanism of acrosomal process elongation. J. Cell Biol. *93*, 820–827.

Tilney, L.G., and Tilney, M.S. (1993). The wiley ways of a parasite: induction of actin assembly by *Listeria*. Trends Microbiol. *1*, 25–31.

Titus, M.A., Wessels, D., Spudich, J.A., and Soll, D. (1993). The unconventional myosin encoded by the *myoA* gene plays a role in *Dictyostelium* motility. Mol. Biol. Cell *4*, 233–246.

Ward, S., Argon, Y., and Nelson, G.A. (1983). Sperm morphogenesis in wild-type and fertilization-defective mutants of *Caenorhabditis elegans*. J. Cell Biol. *91*, 26–44.

Wessels, D., Murray, J., Jung, G., Hammer, J.A., and Soll, D.R. (1991). Myosin 1B null mutants of *Dictyostelium* exhibit abnormalities in motility. Cell Motil. Cytoskel. *20*, 301–315.

Zigmond, S.H. (1993). Recent quantitative studies of actin filament turnover during cell locomotion. Cell Motil. Cytoskel. *25*, 309–316.